

# Aggregating Large Wind Farm Composed of Different Smaller Wind Farms

Dr.Ahmed M. Atallah

Atallah\_eg@yahoo.com

Elect. Power & Machine Dept., Faculty of Eng  
Ain-Shames Univ., Cairo, EGYPT

Eng.Mona A. Bayoumi

Eng\_mona\_25@yahoo.com

Elect. Power & Machine Dept., Faculty of Eng.  
Banha Univ., Cairo, EGYPT

**Abstract** – This paper presents a comprehensive dynamic equivalent model of a wind farm with doubly fed induction generator wind turbine using back to back converter. This paper uses a wind farm with different wind turbines (same wind turbine technology but different rated power) coupled to the same grid connection point. It presents a comparative study of four aggregated modeling techniques, namely, full aggregated model using equivalent wind speed (FAM-EWS), full aggregated model using average wind speed (FAM-AWS), semi aggregated model (SAM), multi full aggregated model using equivalent wind speed (MFAM-EWS). Simulation has been carried out for these techniques and compare them with the complete model using their different effects such as wind farm power, reactive power and system dynamics; besides varying the variance effects on these techniques.

**Keywords** - Wind farm aggregation, dynamic wind farm model, wind speed variance and doubly fed induction generators.

## Symbols and Abbreviations

MFAM-EWS	multi full aggregated model using equivalent wind speed
FAM-EWS	full aggregated model using equivalent wind speed
FAM-A	full aggregated model using average wind speed
SAM	semi aggregated model(SAM)
DFIG	doubly fed induction generator
AWF	aggregated wind farm
$P_w(W)$	the aerodynamic power
$(kg/m^3)$	the air density
$A(m^2)$	the rotor disk area
$R(m)$	the rotor radius
$u(m/s)$	the wind speed
$C_p$	the turbine coefficient of performance
	the tip speed ratio
	the pitch angle of rotor blades
$T_{wt}$	the mechanical torque from the wind turbine rotor shaft
$T_m$	the mechanical torque from the generator shaft
$T_g$	the generator electrical torque
$H_r$	the rotor inertia

$H_g$	the generator inertia
$K_m$	the stiffness of the mechanical coupling
$D_m$	the damping of the mechanical coupling
$u$	denotes voltage
$i$	denotes current
index d	the direct components
index q	the quadrature components
index s	refers to stator
index r	refers to rotor
$e'_d, e'_q$	internal voltage components of induction generator
$s$	the synchronous speed
$s$	the generator slip
$T'_o$	the transient open circuit time constant
$X_s$	the stator reactance
$X'_s$	the transient reactance
$R_s$	the stator resistance
$R_r$	the and rotor resistance
$L_{\sigma s}$	the stator leakage inductance
$L_{\sigma r}$	the rotor leakage inductance
$L_m$	the magnetizing inductance
NWS	nominal wind speed
OPTS	the optimal tracking strategy

## I. INTRODUCTION

Wind energy has the potential to play an important role in future energy supply in many areas of the world. The growing worldwide market will lead to further improvements, such as larger wind turbines or new system applications (e.g. offshore wind farms). These improvements will lead to further cost reductions and the wind energy will be able to compete with conventional fossil fuel power generation technology [1]. With the increasing amount of wind power penetration in power systems; wind farms begin to influence power systems. This justifies the need of adequate models for wind farms in order to represent overall power system dynamic behavior for grid connected wind farms.

There are different wind turbine generators types are currently widely applied in wind power today. The main comparison can be made between fixed speed and variable speed wind generator concepts. The directly grid coupled squirrel cage induction generator, used in fixed speed wind turbines. The two variable speed wind generator concepts are

the doubly fed induction generator and the converter driven synchronous generator [2]. Doubly fed induction generators (DFIGS) wind turbines are largely deployed in wind farms due to their advantages such as: the variable speed generation, the decoupled control of active and reactive powers, the reduction of mechanical stresses, less noise, improvement of power quality, and use of smaller power converter (rated power of only 25% of total wind system power).

A wind farm contains a large number of individual wind turbine generators, possibly exceeding 100 of wind turbines. Modeling each of these wind turbine generators separately increases the complexity and compromises the simulation speed significantly. A complete wind farm model with  $n$  number of wind turbines equipped with doubly fed induction generator (DFIG) is shown in Figure (1). The complete wind farm model can be simplified by using an aggregated wind farm (AWF) model, which reduce the size of the power system model, the data requirement and the simulation computation time. This aggregated model can first represent the behavior (active and reactive power exchanged with the grid) during normal operation, characterized by small deviations and the changes of wind speed. Secondly, it represents the behavior of wind farm during grid disturbances, such as voltage drops and frequency deviations [3].

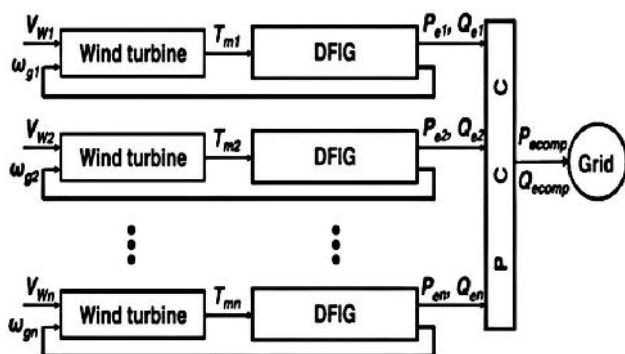


Figure (1): Block diagram of a complete DFIG wind farm model

In this paper we have chosen four aggregating techniques and compared them with complete model as a reference. These techniques are:

- 1- FAM-AWS [3].
- 2- FAM-EWS [4].
- 3- SAM [5].
- 4- MFAM-EWS.

The full aggregated model of wind farms with DFIG wind turbines represent the whole wind farm by one single equivalent wind turbine without using a dynamic simplified model of each individual wind turbine. It consists of one equivalent wind turbine and one equivalent generator for a wind farm with average wind speed or with equivalent wind speed as shown in Figure (2a) The equivalent wind speed can be obtained by getting the output power of each wind turbine

which is derived from its power curve corresponding to the incoming wind. The equivalent power is obtained by the sum of the output power of all wind turbines power. Assuming the per unit power curve of the equivalent wind turbine is equal to that one of the individual wind turbine; the equivalent wind can be calculated from the equivalent power, using the equivalent wind speed power curve. The semi aggregated model is based on using a dynamic simplified model of each individual wind turbine to approximate the generator mechanical torque according to the incoming wind. The generator mechanical torques of each individual wind turbines is aggregated and the resulting torque is applied to an equivalent generator system as shown in Figure (2b). In MFAM-EWS we split the wind turbines on the farm to some smaller farms. Each small farm composed of identical wind turbines. Then we get the full aggregated model using equivalent wind speed for each small farm. Finally, we sum up powers (active and reactive) to get the total farm powers. So in this technique the wind farm is modeled with more than one equivalent wind turbine [6].

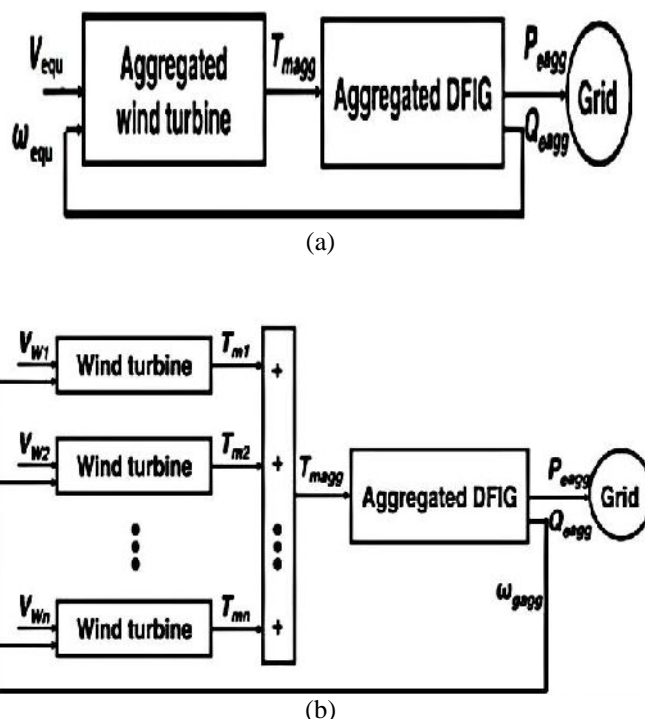


Figure (2): Block diagram of (a) full aggregated and (b) semi aggregated DFIG wind farm models

Also we have compared the active power using these techniques for different speed variances (speed variances are taken as 0.1, 0.5, and 1) where the whole wind farm have the same variance in each case as shown in Figure (3(a,b,c)). We can conclude that the effect of variance on the closeness of any aggregated method to the complete solution cannot be seen. The same results are found in Figure (4(a,b,c)) when comparing reactive powers.

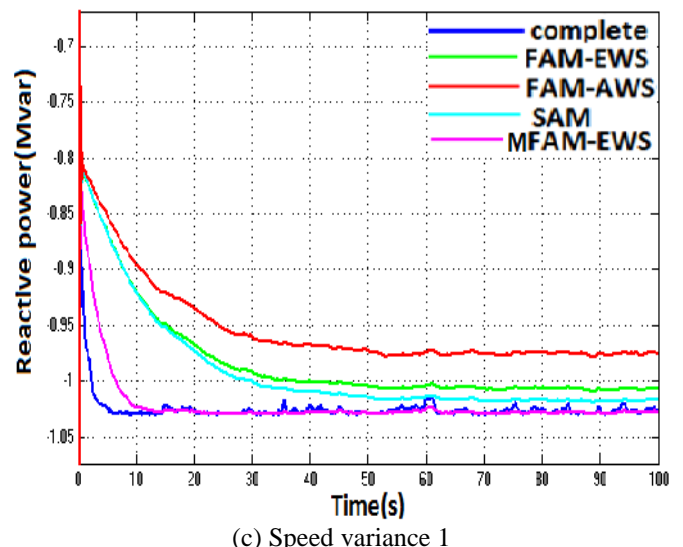
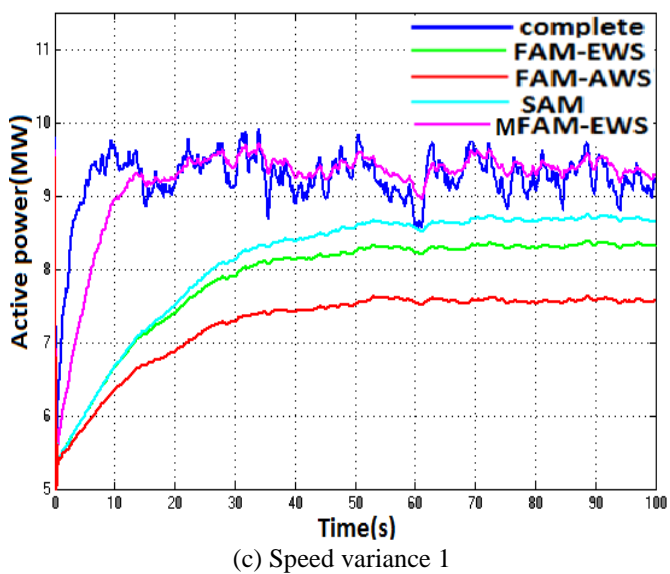
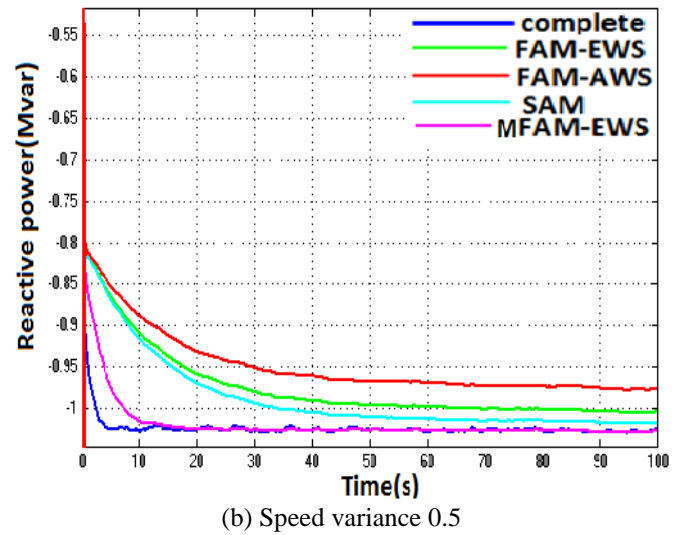
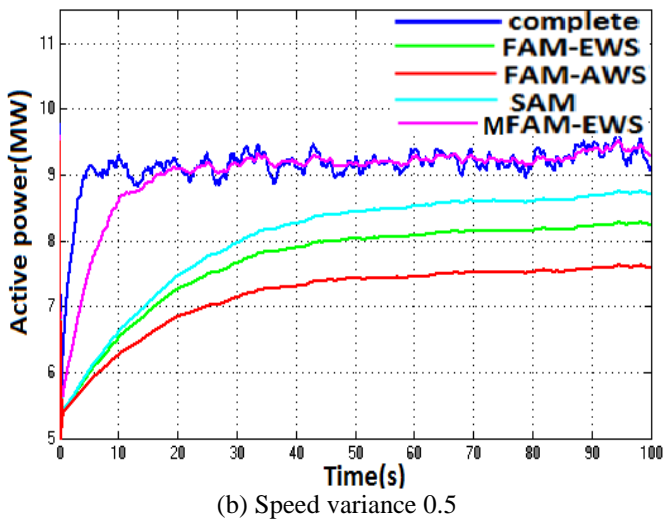
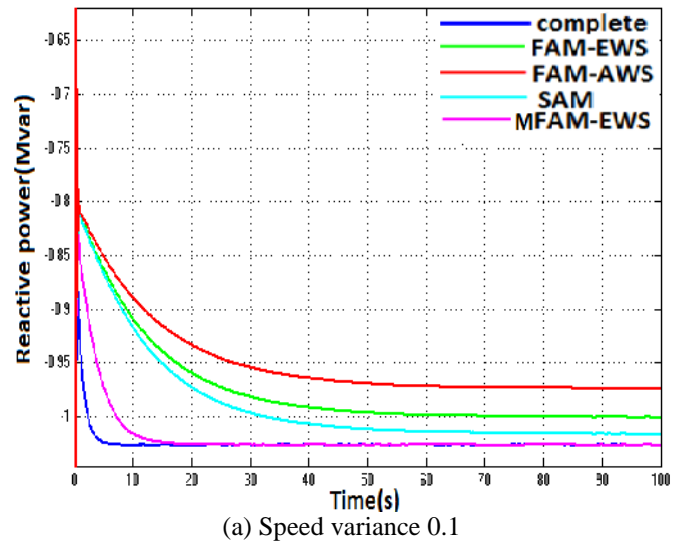
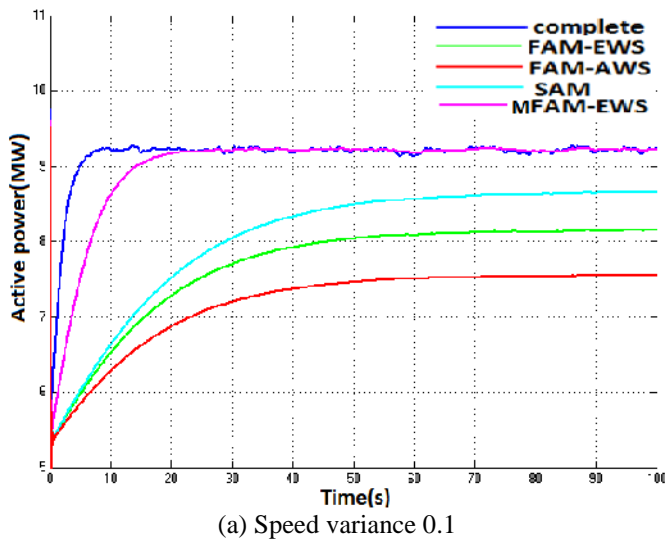


Figure (3): Active power with different variance speed

Figure (4): Reactive power with different variance speed

## II. COMPLETE WIND FARM MODEL

As shown in Figure (5) a DFIG wind farm contains a large number of DFIG wind turbines operating at an internal electrical network (lines and transformers) which enables the generated power to be delivered to grid. A complete model represents dynamic response of a DFIG wind farm, in which all the wind turbines and internal electrical network are modeled.

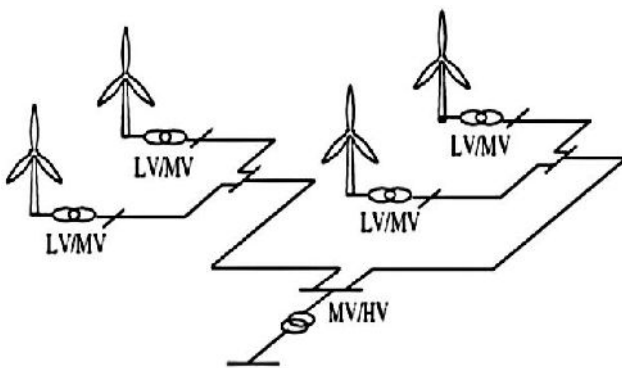


Figure (5): DFIG wind farm

### A. DFIG Wind Turbine

The basic configuration of a DFIG wind turbine is depicted in Figure (6). The most significant feature of this kind of wound-rotor machine is that it has to be fed from both stator and rotor side. Normally, the stator is directly connected to the grid and the rotor is interfaced through a variable frequency power converter. This power converter made of two back to back IGBT bridges based voltage source converters linked by a DC bus. It decouples the electrical grid frequency and the mechanical rotor frequency, thus enabling variable speed wind turbine generation. In high wind speeds, the power extracted from the wind can be limited by pitching the rotor blades. [2].

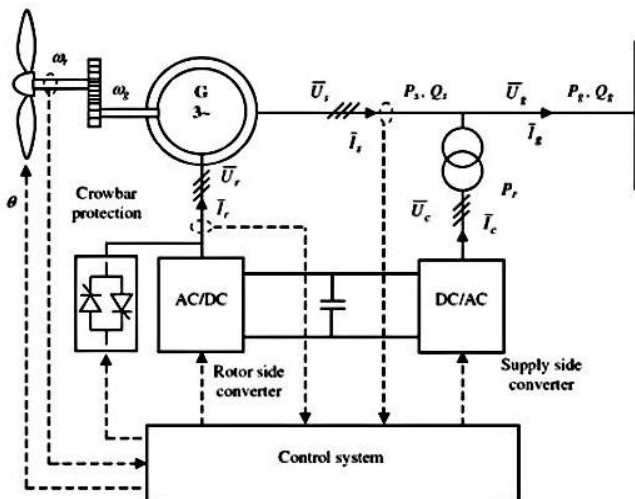


Figure (6): DFIG wind turbine

The DFIG wind turbine has been represented by modeling the rotor, drive train, induction generator, power converter and the protection system. The parameters of the DFIG wind turbine used in this paper are shown in Table 1 [7].

Table 1. DFIG wind turbine parameters

Parameter	Symbol	Value	Unit
Nominal mechanical output power	$P_{mec}$	1.5	MW
Nominal electrical power	$P_e$	1.5/9	MW
Nominal voltage (L-L)	$V_{nom}$	575	V
Stator resistance	$R_s$	0.00706	p.u.
Stator leakage inductance	$L_s$	0.171	p.u.
Rotor resistance	$R_r$	0.0058	p.u.
Rotor leakage inductance	$L_r$	0.156	p.u.
Magnetizing inductance	$L_m$	2.9	p.u.
Base frequency	$f$	60	Hz
Inertia constant	$H$	0.84	s
Friction factor	$F$	3	p.u.
Pair of poles	$p$	0.01	-

### 1. Rotor model

The wind power  $P_w$  captured by the wind turbine is given by [2].

$$P_w = 0.5 \rho A u^3 c_p(\lambda, \theta) \quad (1)$$

The power extracted from the wind is maximized if the rotor speed is such that  $C_p$  is maximum, which occurs for a determined tip speed ratio.

### 2. Drive train model

The drive train of DFIG wind turbine has been represented in this paper by the two masses model [2]:

$$T_{wt} - T_m = 2H_r \frac{d\omega_r}{dt} \quad (3)$$

$$T_m = D_m(\omega_r - \omega_g) + K_m \int (\omega_r - \omega_g) dt \quad (4)$$

$$T_m - T_g = 2H_g \frac{d\omega_g}{dt} \quad (5)$$

### 3. Generator model

Basically, DFIG is an induction type generator. The equivalent circuit of DFIG is shown in Figure (7).

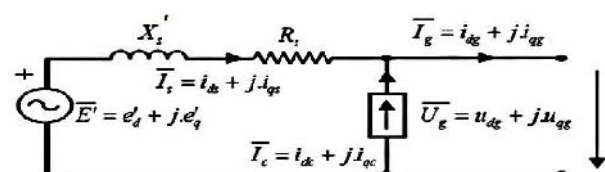


Figure (7): Equivalent circuit of DFIG wind turbine

The wound rotor induction generator has been represented by the third-order model for stability transient studies of power systems. This model is obtained by neglecting the stator transients for the fifth order model of induction generator. It presents three differential equations [8]: two are electrical equations and the third equation is mechanical, given by (5). The model is expressed into a direct and quadrature reference frame rotating at synchronous speed with the position of the direct axis aligned with the maximum of the stator flux. It enables the decoupled control of active and reactive powers of DFIG [9]. Equations (6-9) are electrical differential expressed per unit and use generator convention, which means that the currents are positive when flowing towards the grid.

$$\frac{de'_d}{dt} = \frac{-1}{T_o} \left( e'_d - (X_s - X'_s) i_{qs} \right) + s\omega_s e'_q - \omega_s \frac{L_m}{L_\sigma + L_m} u_{qr} \quad (6)$$

$$\frac{de'_q}{dt} = \frac{-1}{T_o} \left( e'_q - (X_s - X'_s) i_{ds} \right) + s\omega_s e'_d + \omega_s \frac{L_m}{L_\sigma + L_m} u_{dr} \quad (7)$$

$$T_g = L_m (i_{ds} i_{qr} - i_{qs} i_{dr}) \quad (8)$$

$$T_o = \frac{L_\sigma + L_m}{L_m}, X_s = \omega_s (L_\sigma + L_m), X'_s = X_s - \omega_s \frac{L_m^2}{L_\sigma + L_m} \quad (9)$$

The bidirectional converter is composed of two back to back IGBT bridges linked by a DC bus. A converter is connected to the rotor winding (rotor side converter) and the other converter to the grid (supply side converter) [10]. The rotor side converter controller aims to control the DFIG active power output for tracking the input power of the wind turbine, and maintains the terminal voltage to the reference value. The active power and voltage are controlled independently via  $u_{qr}$  and  $u_{dr}$ , respectively. The grid side converter controller aims to maintain the DC link voltage, and control the terminal reactive power [9].

#### 4. Control system

The control of DFIG wind turbine is consist of three controllers: rotor speed, blade pitch angle and reactive power controller as shown in Figure (8(a,b,c)). The control of wind turbine is based on the following control strategies [9]:

1. Power optimization below rated wind speed. In this case, the wind turbine generates the optimum power corresponding to the maximum power coefficient. The blade pitch angle controller keeps the pitch angle to its optimal, whereas the tip speed ratio is driven to its optimal value by the rotor speed controller acting on the rotor speed/generator torque.
2. Power limitation above rated wind speed. The wind turbine operates with the power limited to the rated value. In this case, the rotor speed controller assures the rated power by

acting on the rotor voltage, whereas the blade pitch angle keeps the generator speed limited to the control value by acting on the pitch angle.

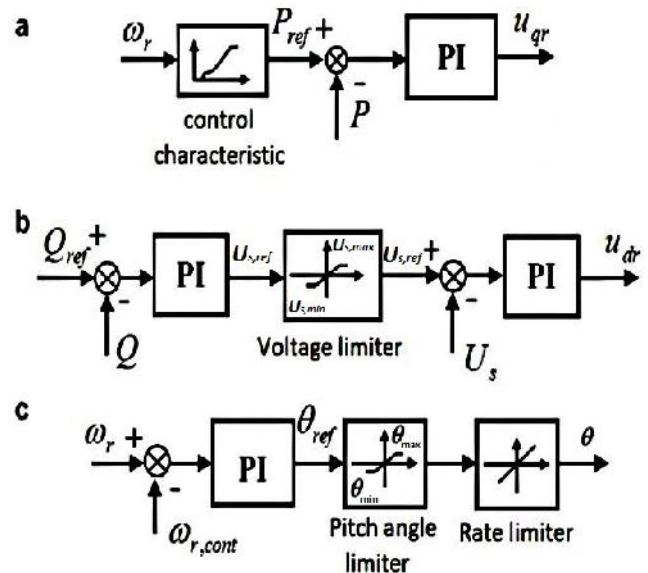


Figure (8): Controllers of a DFIG wind turbine: (a) rotor speed controller, (b) reactive power controller and (c) blade pitch angle controller

#### B. Wind Farm Electrical Network

The wind farm electrical network is modeled by the static model of electric lines and transformers, represented by constant impedance, as usual for power systems simulations [8].

A matlab simulation has been done to present the proposed systems.

### III. POWER CURVE OF DFIG WIND TURBINE

The power curve of the DFIG wind turbine model from SimPowerSystems is shown in Figure (9) [10]. Each point on the power curve represent three values, turbine output power, wind speed, and turbine speed. By the ABCD curve, from zero speed to speed of point A the mechanical power of the DFIG is zero. Between point A and point B the curve is introduced to smooth the power fluctuations occurring near point A. Between point B and point C, DFIG uses the optimal tracking strategy (OPTS) to capture maximum wind energy during the incoming wind speed which is less than the nominal wind speed (NWS). When incoming wind is greater than NWS, the blade pitch control is used to reduce the mechanical power to the equipment rating, which corresponds to the horizontal line starting from D. Between point C and point D the curve is introduced to smooth the power fluctuations occurring near NWS.

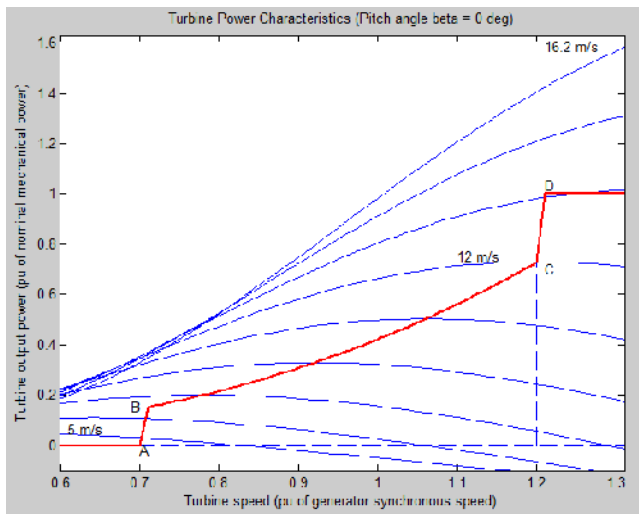


Figure (9): Power curve of DFIG from SimPowerSystems

Table 2 shows the data regarding the four points A-D of the power curve.

Table 2. Data of point A-D

Points	Wind speed (m/s)	Turbine speed (p.u.)	Turbine output power (p.u.)
A	4.23	0.7	0
B	7.1	0.71	0.151
C	12	1.2	0.73
D	13.48	1.21	1

#### IV. EQUIVALENT WIND METHOD (EWM)

The EWM from [11] is used for the aggregation of DFIG wind turbines. This equivalent wind is derived from the power curve of the wind turbine, according to the following procedure:

1. The output power of each wind turbine  $P_j$  is derived from its power curve corresponding to the incoming wind.

$$P_j^{wt} = PC_{wt}(v_j) \quad (10)$$

where  $PC_{wt}(v_j)$  is a function which represents the power curve of the wind turbine against wind speed and the super index  $wt$  represents the value in p.u., expressed in the individual wind turbine base.

2. The equivalent power  $P_{eq}$  is the sum of the output power of all wind turbines power,

$$P_{eq}^{wt} = \sum_{j=1}^n P_j^{wt} \quad (11)$$

3. After that,  $P_{eq}^{wt}$  is expressed in the equivalent wind turbine base as  $P_{eq}^{ewt}$ . Where the resulting power curve expressed in the equivalent wind turbine base is the same as the individual wind turbines,

$$P_{eq}^{ewt} = PC_{ewt}(v_{eq}) \quad (12)$$

$$PC_{ewt} = PC_{wt} \quad (13)$$

4. The equivalent wind speed of the whole aggregated system is derived from the inverse function of the power curve.

$$v_{eq} = PC_{ewt}^{-1}(P_{eq}^{ewt}) \quad (14)$$

5. If all aggregated DFIG wind turbines faced above nominal winds, the equivalent wind is the average wind speed.

#### V. SIMULATIN RESULTS

The overall system is shown in Figure (10). A wind farm from SimPowerSystems has been used for simulation studies. The wind farm consists of nine wind turbines connected to a 25 kV distribution system, and a 500 kW load is connected on the 575 V bus of the wind farm. The parameters of this studies system can be found in [7].

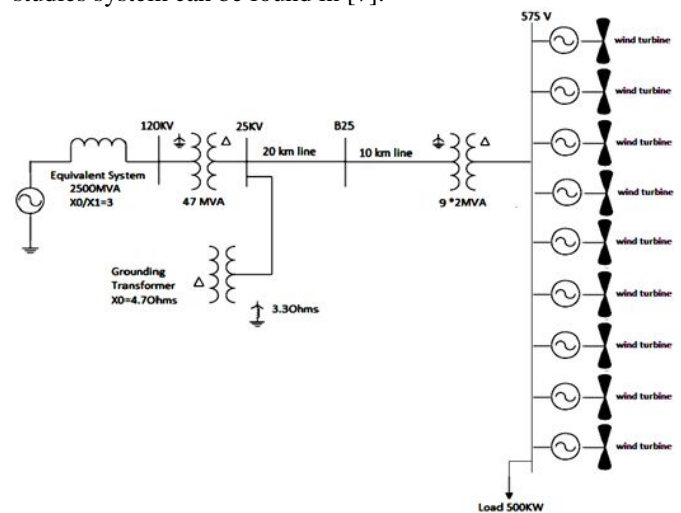


Figure (10): A wind farm connected to a distributed system

The complete, FAM-AWS, FAM-EWS, SAM, and MFAM-EWS are simulated using Matlab software to obtain the dynamic responses at the PCC under the following two conditions: 1- normal operation and 2- grid disturbance. The variables considered for the comparison are the active ( $P_e$ ) and reactive power ( $Q_e$ ) exchange between the wind farm and power system. During normal operation, all wind turbine operate under wind fluctuations. Two cases are presented, case 1 using wind turbines with the same rated power and

case 2 using wind turbines with different rated power . Table 3 shows the speed of the wind received by the DFIG wind turbines.

Table 3. Wind speeds incident on the wind turbines

Wind turbine	Wind speed (m/s)
WT1	8.7
WT2	6.9
WT3	7.3
WT4	10.5
WT5	7.7
WT6	8.5
WT7	9.5
WT8	10.8
WT9	11

A. Case 1

1. Normal Operation

A 13.5 MW wind farm has been used for simulation studies. The wind farm consists of nine 1.5MW wind turbines. During normal operation, the wind farm operates under wind speed fluctuations. The wind farm has been simulated with different incoming winds. In this case, the technique MFAM-EWS behaviour the same as FAM-EWS in the case of farm composed of only identical wind turbines so we will satisfy with the results of FAM-EWS. The collective responses of the complete, two full aggregated and semi aggregated wind farm models at the PCC during normal operation are shown in Figure (11).

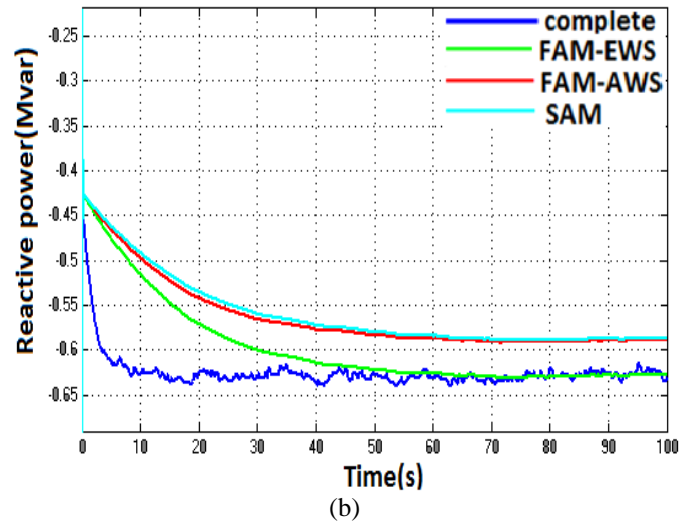
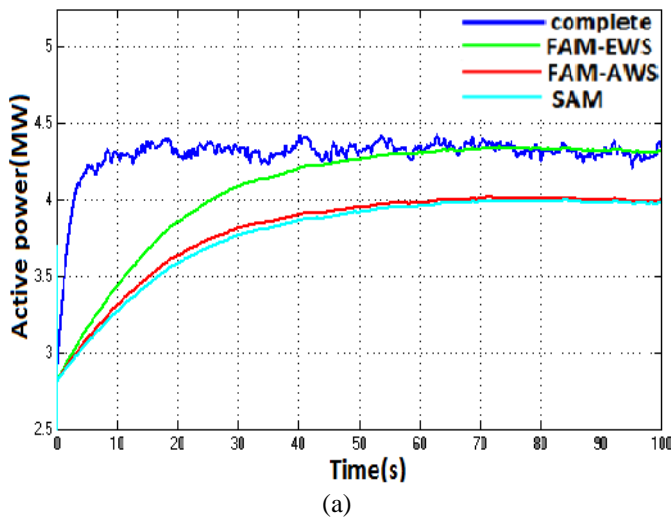
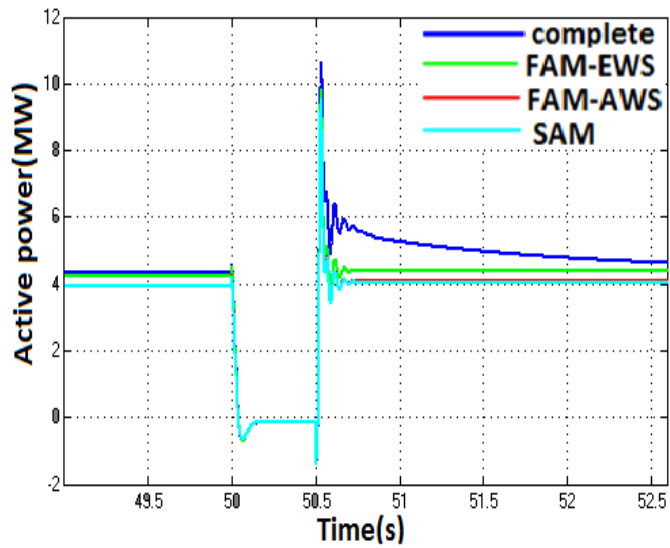


Figure (11): (a) Active power at PCC during normal operation, (b) Reactive power at PCC during normal operation

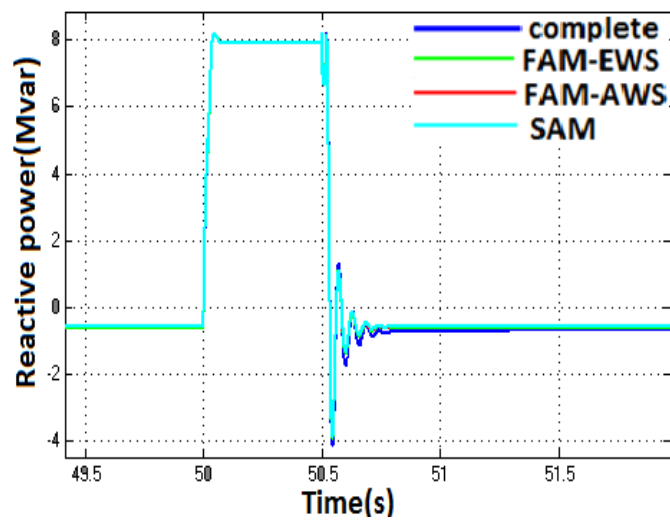
The results depicted in Figure (11) shows that FAM-EWS or MFAM-EWS has a higher correspondence in approximating active and reactive power to the complete model. Unlike in ref [3] where he proposed aggregation technique with the incorporation of a mechanical torque compensation factor into the full AWF model. They compare between FAM-AWS and SAM. But he did not use the FAM-EWS technique which gives better and closer results to the complete technique.

2. Grid Disturbances

A voltage sag of 50% lasting for 500 ms is originated at the PCC at t = 50 s. Evaluating the collective responses of the complete, two full aggregated and semi aggregated wind farm models during grid disturbances at PCC gives the results shown in Figure (12).



(a)



(b)

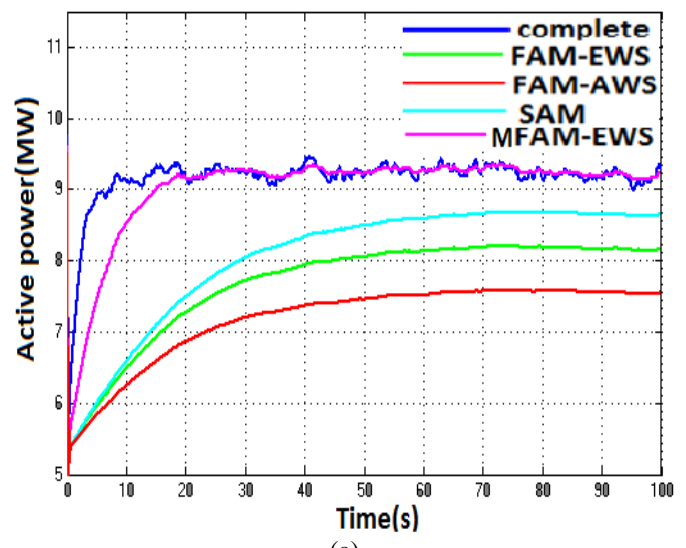
Figure 12: (a) Active power at PCC during grid disturbance, (b) Reactive power at PCC during grid disturbance

From Figure 12(a,b) we can conclude again that FAM-EWS or MFAM-EWS is also much closer to the complete model during the simulation of grid disturbances. This means that we can rely on FAM-EWS even at cases of system dynamic disturbances.

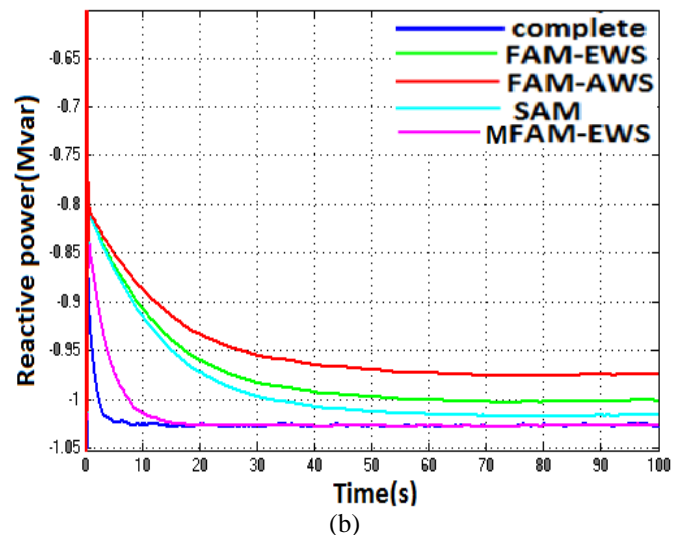
## B. Case 2

### 1. Normal Operation

A 25.5 MW wind farm has been used for simulation studies. The wind farm consists of three 1.5 MW, three 3 MW, and three 4 MW wind turbines. The collective responses of the complete, FAM-AWS, FAM-EWS, SAM, and MFAM-EWS at the PCC during normal operation are shown in Figure 13).



(a)



(b)

Figure 13: (a) Active power at PCC during normal operation, (b) Reactive power at PCC during normal operation

Figure 13) shows that MFAM-EWS has a higher correspondence in approximating active and reactive power to the complete model than the whole other techniques for wind farm consist of different wind turbines.

### 2. Grid Disturbances

A voltage sag of 50% lasting for 500 ms is originated at the PCC at  $t = 50$  s. Evaluating the collective responses of the complete, FAM-AWS, FAM-EWS, SAM, and MFAM-EWS during grid disturbances at PCC gives the results shown in Figure 14).



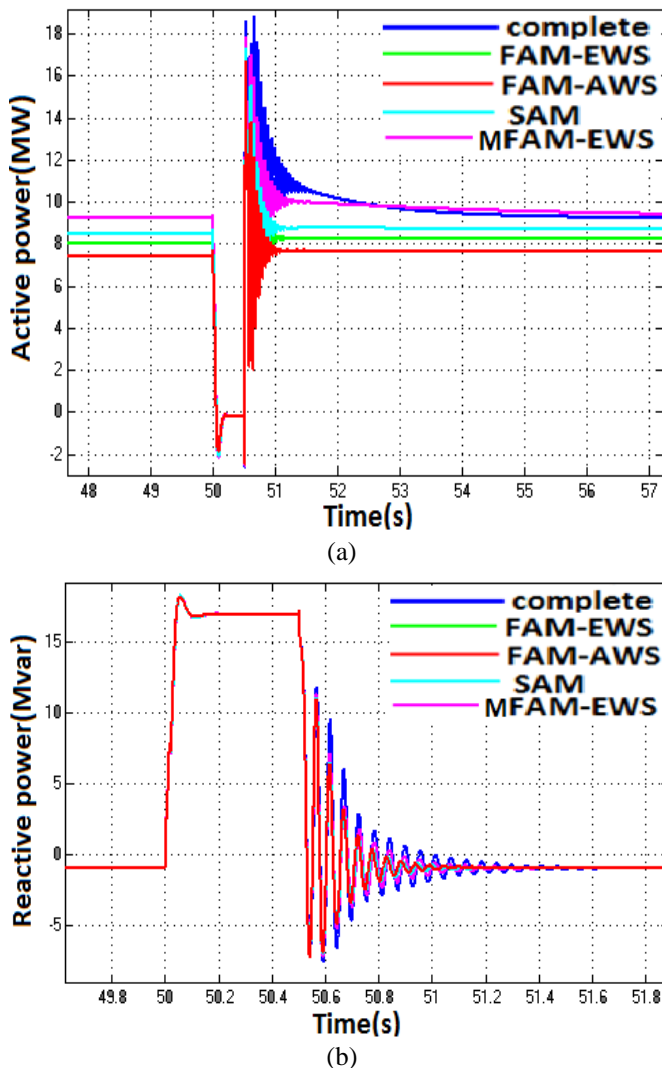


Figure 14): (a) Active power at PCC during grid disturbance,  
 (b) Reactive power at PCC during grid disturbance

From Figure (14) we can conclude that MFAM-EWS is also much closer in the results of the other three aggregated models during the simulation of grid disturbances.

From Figures (11) to (14) it is clear that the MFAM-EWS is the closest results to the complete model in both cases, farm composed of identical wind turbines (case 1) and farm composed of different wind turbines (case 2). SAM is the second closest model in case 2 and gives closer results than FAM-EWS. But MFAM-EWS gives the first closest results.

## VI. CONCLUSION

This paper presented four aggregated models of variable speed wind farms equipped with DFIG wind turbines. In this paper, a comparison between complete, two full aggregated, semi aggregated and multi full aggregated model using

equivalent wind speed models are simulated using Matlab simulation program. First, we examine the effect of varying the variance of the applied wind speeds on different proposed aggregated models and we found that no clear evidence that varying the variance affects differently on different aggregated models. Second, the full aggregated model using equivalent wind speed is closer to the complete model in the case of a wind farm of the same rated power of wind turbines. But in the case of wind farm composed of wind turbines with different rated power, multi full aggregated model using equivalent wind speed gives the accurate approximation of the collective responses at the PCC during normal operation and grid disturbances.

## REFEERNCES

- [1] T. Ackermann, Ed., *Wind Power In Power Systems*, 2nd ed. John Wiley & Sons, 2012.
- [2] L.M. Fernández, J. R. Saenz, and F. Jurado, *Aggregated dynamic model for wind farms with doubly fed induction generator wind turbines*, *Renewable Energy*, vol. 33, pp. 129–140, 2008.
- [3] M.A. Chowdhury, W.X. Shen, N. Hosseinzadeh, and H.R. Pota, *A novel aggregated DFIG wind farm model using mechanical torque compensating factor*, *Energy Conversion and Management*, vol 67, pp.265–274, 2013.
- [4] Z. J. Meng, and F. Xue, *Improving the Performance of the Equivalent Wind Method for the Aggregation of DFIG Wind Turbines*, *IEEE, Power and Energy Society General Meeting*, pp. 1-6, 2011.
- [5] M. A. Chowdhury, N. Hosseinzadeh, M. M. Billah and S. A. Haque, *Dynamic DFIG wind farm model with an aggregation technique*, *ICECE 2010*, 18-20 December 2010, Dhaka, Bangladesh.
- [6] M. Ali, I.-S. Ilie, J.V. Milanovic and G. Chicco, *Probabilistic clustering of wind generations*, *Proc. IEEE PES General Meeting*, pp. 1-6, 2010.
- [7] SimPowerSystems, User's guide, Natick, MA: The Mathworks Inc., 2011.
- [8] Heier S, *Grid integration of wind energy conversion systems*, Chichester, Wiley, 1998.
- [9] Ekanayake JB, Holdsworth L, Wu X, and Jenkins N, *Dynamic modeling of doubly fed induction generator wind turbines*, *IEEE Trans Power Syst*, 18(2): 803–9, 2003.
- [10] L. M. Fernandez, C. A. Garcia, J. R. Saenz, and F.Jurado, *Equivalent models of wind farms by using aggregated wind turbines and equivalent winds*, *Energy Conversion and Management*, vol. 50, pp. 691–704, 2009.
- [11] L. M. Fernandez, C. A. Garcia, J. R. Saenz, and F.Jurado, *Reduced model of DFIGs wind farms using aggregation of wind turbines and equivalent wind*, *IEEE MELCON*, pp. 881–884, 2006.